OPEN ACCESS
CellPress

Cell Reports
Article

MicroRNA Targeting of CoREST Controls Polarization of Migrating Cortical Neurons

Marie-Laure Volvert,[1,3] Pierre-Paul Prévot,[1,3] Pierre Close,[2,3] Sophie Laguesse,[1,3] Sophie Pirotte,[1,3] James Hemphill,[5,6] Florence Rogister,[1,3] Nathalie Kruzy,[1,3] Rosalie Sacheli,[1,3] Gustave Moonen,[1,3] Alexander Deiters,[5,6] Matthias Merkenschlager,[7] Alain Chariot,[2,3,4] Brigitte Malgrange,[1,3] Juliette D. Godin,[1,3] and Laurent Nguyen[1,3,4,*]

[1]GIGA-Neurosciences
[2]GIGA-Signal Transduction
[3]Interdisciplinary Cluster for Applied Genoproteomics (GIGA-R)
[4]Walloon Excellence in Lifesciences and Biotechnology (WELBIO)
University of Liège, C.H.U. Sart Tilman, Liège 4000, Belgium
[5]Department of Chemistry, North Carolina State University, Raleigh, NC 27695, USA
[6]Department of Chemistry, University of Pittsburgh, Pittsburgh, PA 15260, USA
[7]Lymphocyte Development Group, MRC Clinical Sciences Centre, Imperial College London, Du Cane Road, London W12 0NN, UK
*Correspondence: lnguyen@ulg.ac.be
http://dx.doi.org/10.1016/j.celrep.2014.03.075

SUMMARY

The migration of cortical projection neurons is a multistep process characterized by dynamic cell shape remodeling. The molecular basis of these changes remains elusive, and the present work describes how microRNAs (miRNAs) control neuronal polarization during radial migration. We show that miR-22 and miR-124 are expressed in the cortical wall where they target components of the CoREST/REST transcriptional repressor complex, thereby regulating doublecortin transcription in migrating neurons. This molecular pathway underlies radial migration by promoting dynamic multipolar-bipolar cell conversion at early phases of migration, and later stabilization of cell polarity to support locomotion on radial glia fibers. Thus, our work emphasizes key roles of some miRNAs that control radial migration during cerebral corticogenesis.

INTRODUCTION

The cerebral cortex comprises six layers of neurons born in the progenitor zones of the forebrain. Dorsal cortical progenitors generate temporal cohorts of neurons that undergo active migration to reach their final positions in successive cortical layers where they extend neurites to finalise contacts with target cells (Bielas et al., 2004; Casanova and Trippe, 2006; Mandel et al., 2011; Marín and Rubenstein, 2003). Cell migration and branching require dynamic cell shape remodeling orchestrated both by extracellular and intracellular cues that ultimately converge on the cytoskeleton (Heng et al., 2010). Not surprisingly, many brain disorders characterized by cortical defects arise through mutations in genes that encode cytoskeletal proteins or their modifiers (Bai et al., 2003; Creppe et al., 2009; Hattori et al., 1994; Keays et al., 2007; Pilz et al., 1998; Sossey-Alaoui et al., 1998). Untangling the mechanisms that drive neuron migration and integration to appropriate neuronal networks is thus critical for understanding the biological basis of these disorders as well as the emergence of cortical architecture, connectivity and functions during development. Although most projection neurons undergo somal translocation at early phases of corticogenesis, they combine different migration modes to reach their final position at later stages (Gupta et al., 2002). Bipolar progenitors leave the ventricular zone (VZ) and start radial migration. When they reach the intermediate zone (IZ), they sprout multiple neurites and become multipolar (Noctor et al., 2004). This morphological conversion is a critical regulation step as mutations in genes that control the multipolar stage often lead to radial migration defects (LoTurco and Bai, 2006). Multipolar-bipolar conversion of projection neurons is further required for appropriate glia-guided locomotion to settle in the cortical plate (Noctor et al., 2004). Over the past few years, several studies started to define the mechanisms underlying radial migration, and most identified regulators were actin or microtubule (MT) cytoskeleton-associated proteins (Heng et al., 2010). In spite of these advances, little is known about the molecular basis and more particularly the epigenetic control of cell shape conversion during the successive steps of radial migration in the cortex.

Epigenetics has recently been extended to the study of microRNAs (miRNAs), which are endogenous single-stranded noncoding small RNAs that induce RNA interference and promote posttranscriptional regulation. MiRNAs regulate signaling pathways that control neurogenesis (Kawahara et al., 2012; Lang and Shi, 2012; Shi et al., 2010) including those that orchestrate successive steps of corticogenesis (reviewed in Volvert et al., 2012). Slight modifications of their expression have been associated with a wide range of brain disorders (Abelson et al., 2005; Hébert et al., 2008; Jimenez-Mateos et al., 2011; Kim et al., 2007; McKiernan et al., 2012; Stark et al., 2008; Wang et al., 2009; Willemsen et al., 2011), some affecting cerebral cortical activity (Aronica et al., 2010; Beveridge et al., 2010; Miller

et al., 2012). Several miRNAs are abundant in the developing cerebral cortex, among which some show dynamic expression that correlates with developmental milestones of the cortex. *Dicer*-null mutants are embryonic lethal in mice (Bernstein et al., 2001). Thus, to bypass early embryonic lethality and analyze miRNA's functions in cerebral cortical development, conditional mouse lines carrying Dicer deletion in telencephalic cells have been established. Experiments performed with these genetic models revealed critical roles for Dicer in cortical neurogenesis (Davis et al., 2008; De Pietri Tonelli et al., 2008; Kawase-Koga et al., 2009; Makeyev et al., 2007; Nowakowski et al., 2011). Although cortical phenotypes resulted from loss of mature miRNAs, functional connections to individual miRNA have been mostly correlative. In addition, miRNA modulations were performed in progenitors, which may have secondary impact on the mobility of projection neurons (Clovis et al., 2012; Gaughwin et al., 2011; Kawase-Koga et al., 2009; Sun et al., 2011). Therefore, there is currently no evidence that miRNAs directly control the migration of postmitotic projection neurons (Volvert et al., 2012).

By combining microarray analyses with conditional deletion of Dicer in newborn projection neurons and time-lapse recording on organotypic brain slices, we identified two miRNAs that control neuronal migration in the developing cortex. Indeed, we showed that, by targeting elements of the CoREST/REST transcriptional repressor complex, miR-22 and miR-124 control the expression of Doublecortin (Dcx), a microtubule-associated protein (MAP) that contributes to the establishment of neuron polarization and radial migration in the cerebral cortex.

RESULTS

Conditional Removal of Dicer in Postmitotic Projection Neurons Impedes Radial Migration

Disruption of *Dicer* in cortical progenitors from $Dicer^{lox/lox}$; $FOXG1^{Cre/+}$ embryos (Cobb et al., 2005; Hébert and McConnell, 2000) resulted in major corticogenesis defects (Figures S1A–S1E), as reported previously (Volvert et al., 2012). Although projection neurons were misplaced (Figure S1D) in the cortical wall, we could not decipher whether Dicer cell autonomously controlled neuronal migration because loss of glial scaffold integrity (Figure S1C), poor cell survival, proliferation, and specification defects (Figures S1B and S1E) secondarily alter radial migration. Therefore, we analyzed embryos that lacked *Dicer* specifically in postmitotic projection neurons. This was achieved by breeding $Dicer^{lox/lox}$ with $NEX^{Cre/+}$ (Goebbels et al., 2006) (termed hereafter Dicer CKO) mice. We assessed the distribution of Satb2-expressing upper-layer neurons in postnatal (P) 2 wild-type (WT) or Dicer CKO cortices. Although most control neurons settled in layers IV to II, numerous Satb2-postive neurons were misplaced in deep layers of Dicer CKO cortex (Figures 1A–1C). We next performed acute deletion of Dicer in a cohort of embryonic day (E) 14 projection neurons by in utero electroporation (Figure 1D) of plasmids expressing Cre and GFP under a regulatory sequence of *NeuroD* (NeuroD:Cre-GFP) or only GFP (NeuroD:GFP) (Figures S2A and S2B). Three days after electroporation, NeuroD:Cre-GFP-expressing neurons selected by fluorescent-activated cell sorting (FACS) and further analyzed by quantitative RT-PCR (RT-PCR) had reduced level of Dicer expression, as compared to control (Figure 1E). Acute removal of Dicer at E14 impaired neuronal migration to upper layers (Figures 1F and 1G) without affecting cell survival (data not shown) or integrity of the glial scaffold (Figure S2C). Large amounts of Cre-electroporated projection neurons were still detected in deep layers after birth (Figures 1H and 1I). Most neurons trapped in deep layers expressed the upper-layer markers Satb2 (layers II–IV; Figure 1K) and Cux1 (layers II–IV; Figure S2D) but not the deep-layer marker Sox5 (layers V and VI; Figure 1J), which supports migration defect rather than laminar specification. It is noteworthy that neurons permanently trapped in deep layers harbored unconventional multipolar shapes at P17 (Figures 1L and 1M). Altogether, these results show that Dicer is cell autonomously required for proper migration of projection neurons to upper layers, and they suggest a direct contribution of miRNAs to radial migration.

Dicer Is Required for Proper Polarization of Newborn Projection Neurons during Migration

Electroporation of cortical progenitors in E14 $Dicer^{lox/lox}$ embryos led to accumulation of GFP-expressing postmitotic (Ki67 negative) neurons (Tbr2 negative) in the intermediate zone (IZ) 2 days later (Figures 2A and 2B). A closer look at the cortical wall revealed accumulation of multipolar cells throughout the IZ (Figures 2C and 2D) and the cortical plate (CP), at the expense of bipolar neurons, after acute removal of Dicer (Figures 2E–2G and S2E). These results prompted us to analyze the dynamic conversion of neuron polarity by real-time imaging (Figure 3A). In utero electroporations of NeuroD:Cre-GFP or NeuroD:GFP constructs were performed in E14 $Dicer^{lox/lox}$ embryos that were further harvested at E16 to set up organotypic brain culture. IZ fields were selected, and GFP-positive neurons were recorded the next day for 10 hr. We analyzed the dynamic multipolar-bipolar conversion of cortical neurons (Figure 3A) and showed that the conditional removal of Dicer impaired this process (Figures 3B and 3D; Movie S1). In addition, some bipolar neurons electroporated with NeuroD:Cre-GFP showed unstable polarity, because they could not maintain bipolar shape during the recording (Figures 3C and 3E; Movie S2). Migration to cortical plate further involves a locomotory phase on radial glia fibers (Figures 3A and 3F–3J). When compared to control projection neurons, Cre-electroporated neurons traveled significantly slower (Figure 3G). However, they underwent long pauses, which almost never occurred in control neurons (Figures 3H and 3I). When pauses were substracted from the analysis, the motility index was comparable in both conditions (Figure 3J). Interestingly, pauses were associated with transient loss of cell polarity and most Cre-expressing neurons were indeed multipolar while pausing (Figures 3K and 3L). In addition, Dicer knockout neurons ended migration by shorter somal translocation (Figures S2F–S2I). Altogether, these results demonstrate that Dicer controls the dynamic polarization of newborn cortical neurons to ensure progression through the successive phases of radial migration (Noctor et al., 2004).

CoREST Overexpression Contributes to Radial Migration Defects of Dicer Conditional Knockout Neurons

Comparative microarray analyses performed on total RNA extracts from E12 $Dicer^{lox/lox}$; $FoxG1^{Cre/+}$ (genetic deletion of

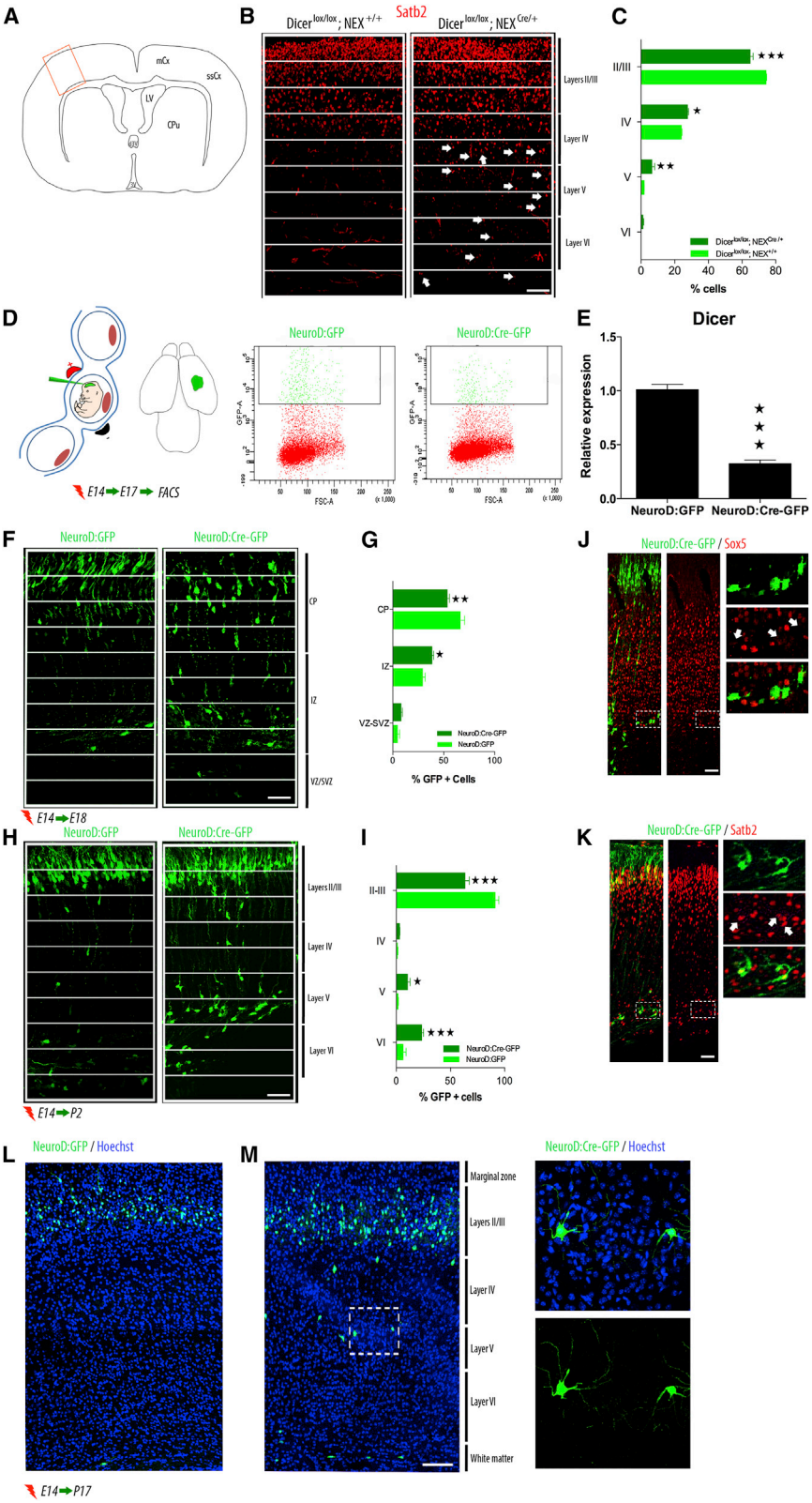

Figure 1. Dicer Expression Is Required for Proper Migration of Projection Neurons

(A–C) Invalidation of Dicer in postmitotic neurons impairs radial migration. Drawing of a postnatal days 2 (P2) brain coronal section (A). Close-up view of the red boxed area in (A) showing the distribution of Satb2-positive (Satb2$^+$) projection neurons in P2 Dicer$^{lox/lox}$, NEX$^{+/+}$, or Dicer$^{lox/lox}$; NEX$^{Cre/+}$ mouse brains. White arrows point electroporated neurons Satb2 positives (red) trapped in deep layers (B). Satb2$^+$ neurons scattering in cortical layers of transgenic mice, genotype as indicated (C).

(D and E) Acute depletion of Dicer in postmitotic projection neurons by in utero electroporation of NeuroD:Cre-GFP-expressing vectors in E14 Dicer$^{lox/lox}$ embryos. In utero electroporation procedure (left) and cortical patch of GFP-expressing neurons (green) 3 days after in utero electroporation (right) further microdissected and FACS purified (grid and gating showing cells of interest in green) (D). Electroporated cells (NeuroD:GFP or NeuroD:Cre-GFP) were subjected to FACS for qRT-PCR analyzes of Dicer expression (E).

(F–K) Acute depletion of Dicer impairs radial migration to upper layers. Cortical scaterring of Dicer$^{lox/lox}$ neurons, 4 (F and G) or 7 (H and I) days after NeuroD:GFP or NeuroD:Cre-GFP in utero electroporation of E14 embryos. Immunolabelings of NeuroD:Cre-GFP electroporated cortex with GFP (green) and deep (Sox5, red) or upper (Satb2, red) layer marker (J and K; 69.44% ± 3.36% of GFP-expressing neurons in deep layers are Satb2+; 2.77% ± 3.14% of GFP-expressing neurons in deep layers are Sox5$^+$; n = 3 brains per condition).

(L and M) Conditional knockout of Dicer in migrating projection neurons leads to permanent defects. Immunolabelings show electroporated cells (GFP, green) with NeuroD:GFP (L) or NeuroD:Cre-GFP (M) in P17 cortex, nucleus counterstaining with Hoechst 33342 (blue). Insets show detailed morphology of a NeuroD:Cre-GFP electroporated neuron trapped in deep layers.

CP, cortical plate; IZ, intermediate zone; VZ/SVZ, ventricular/subventricular zones; FACS, fluorescent-activated cell sorting. Scale bars, 100 μm in (B), (F), (H), (J), and (K) and 200 μm in (M). See also Figure S1.

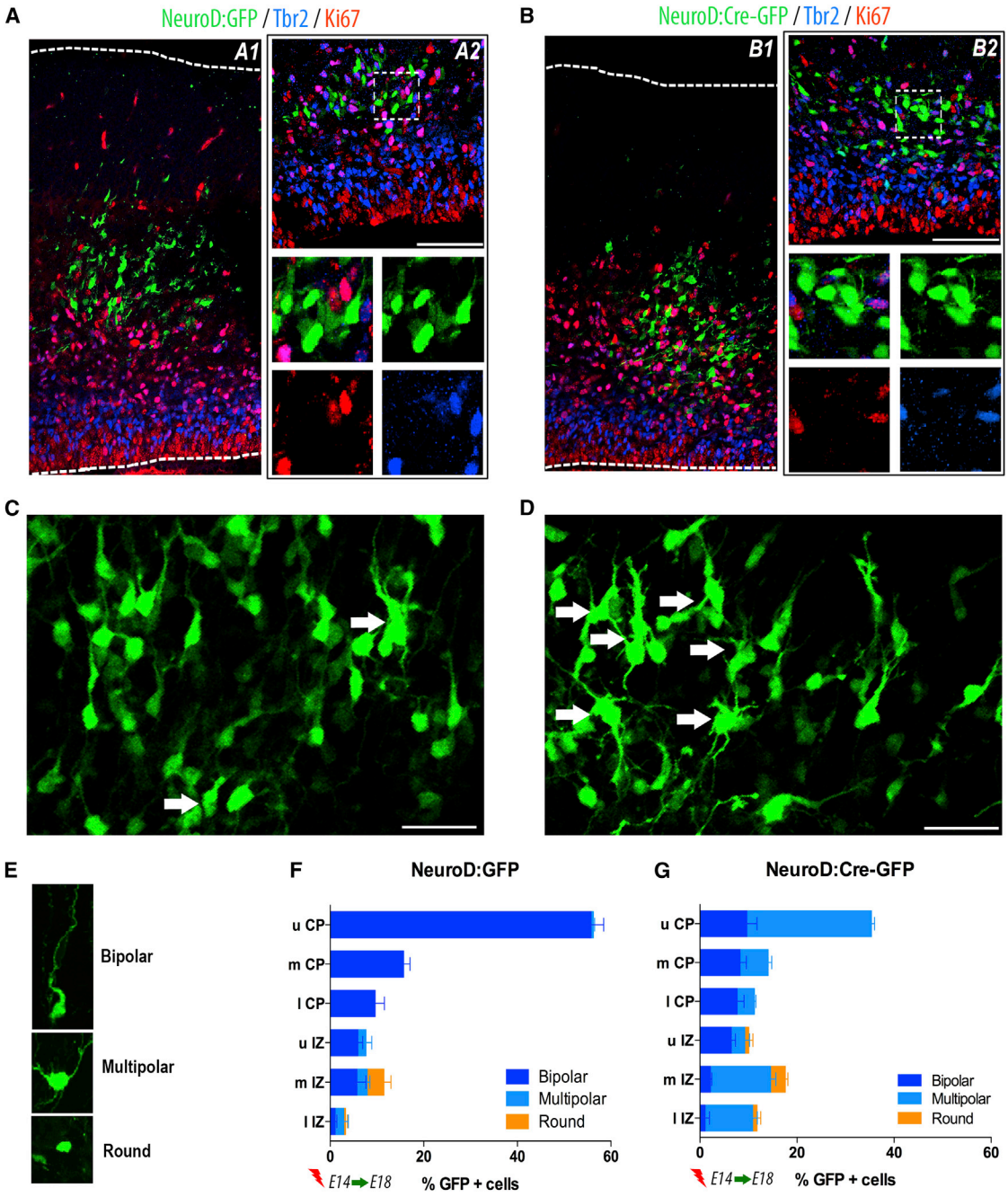

Figure 2. Accumulation of Multipolar Cells throughout the Cortical Wall of Dicer Conditional Knockout Neurons

(A–D) Immunolabelings of brain sections from disctinct Dicer$^{lox/lox}$ E16 embryos electroporated 2 days earlier with NeuroD:GFP (A1 and A2) or NeuroD:Cre-GFP plasmids (B1 and B2). Most electroporated neurons express GFP (green) but not Tbr2 (blue) nor Ki67 (red) (99.69% ± 0.27% for NeuroD:GFP and 98.77% ± 1.07% for NeuroD:Cre-GFP; n = 3 brains per condition, see magnified field in A2 and B2) (A and B). Electroporated neurons exhibit multipolar morphology (white arrows) in the intermediate zone (IZ) of the cortical wall (C and D). Accretion of multipolar neurons after electroporation of NeuroD:Cre-GFP (D) but not NeuroD:GFP (C).

(E–G) Migrating projection neurons have different morphologies (E) after electroporation with NeuroD:GFP (F) or NeuroD:Cre-GFP (G).

uCP, upper; mCP, median; lCP, lower cortical plates; ulX, upper; mIZ, median; and lIZ, lower intermediate zones. Scale bars, 100 μm in (A2) and (B2) and 50 μm in (C) and (D).

Dicer in telencephalic cells) and WT cortices allowed the identification of some differentially expressed genes that control neuronal polarity in the cerebral cortex (Heng et al., 2008; LoTurco and Bai, 2006; Mandel et al., 2011). Selected candidates, including *FoxP2* (1.92-fold increase in Dicer knockout backround), *REST* (1.94-fold increase), *CoREST* (2.11 fold

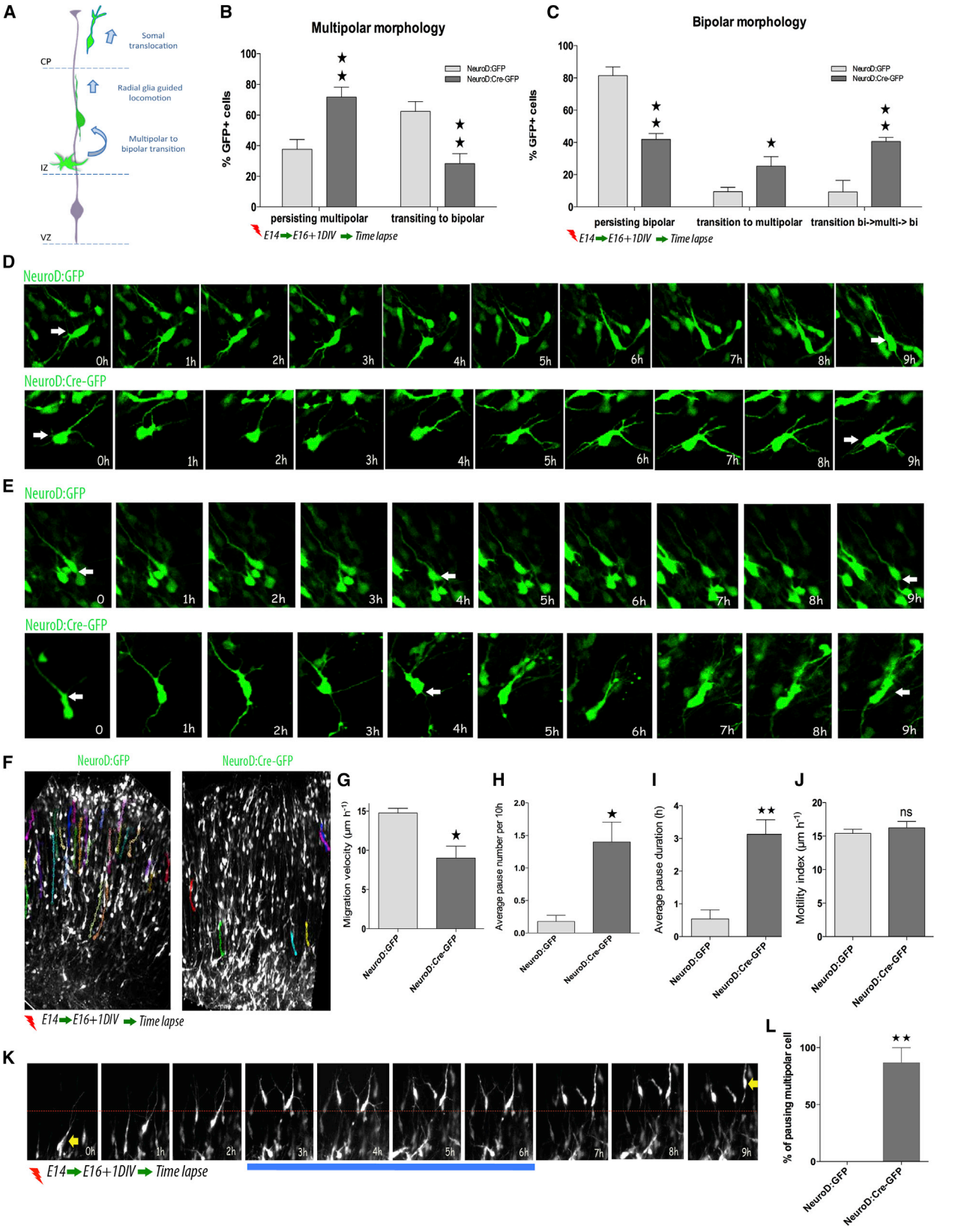

(legend on next page)

increase), and *Rnd2* (2.32-fold decrease), were analyzed by qRT-PCR on RNA extracts from FACS-purified neurons from E17 Dicer$^{lox/lox}$ embryos electroporated in utero with NeuroD:Cre-GFP or NeuroD:GFP at E14. CoREST, a corepressor that associates with the transcriptional repressor REST (Ballas et al., 2005), was the only candidate from our short list (Figures 4A and S3A–S3D) or from published work (stathmin [Westerlund et al., 2011], neuropilin-1 [Chen et al., 2008], and COUP-TF1 [Alfano et al., 2011]) (Figures S3E–S3H) whose expression was significantly affected. It is noteworthy that the methyl CpG binding protein 2 (MeCP2), an additional component of the CoREST/REST repressor complex, was also slightly increased in Dicer-depleted neurons (Figure S3I). CoREST is indeed a strong candidate because it regulates radial migration (Fuentes et al., 2012), and its protein expression level decreases between E14 and birth in the cortex, when most projection neurons reach their dedicated cortical layer (Figure 4B). These results were further supported the faint detection of CoREST in the IZ, a cortical region enriched in migrating neurons (Figure 4C). It is noteworthy that CoREST expression was heterogenous throughout the CP, with higher expression in early-born Ctip2-expressing neurons that halted migration in deep layers, as compared to upper-layer neurons (Satb2 positives) (Figure 4D). Importantly, coelectroporating NeuroD:Cre-GFP and CoREST small hairpin RNA (shRNA) targeting vectors in Dicer$^{lox/lox}$ neurons normalized CoREST expression to basal level (Figure S3J) and rescued neuronal polarization (Figures 4E and 4F) and migration defects (Figures 4G and 4H) without reducing CoREST expression in cortical progenitors (Figure S3N). On the other hand, in utero expression of CoREST in postmitotic neurons using NeuroD:CoREST vectors impaired their migration in the cortex (Figures S3L and S3M). Altogether, our results suggest that (1) a tight regulation of CoREST expression by miRNAs is required for appropriate polarization and migration of projection neurons in the developing cortex; (2) CoREST accumulates in postmitotic neurons that reached their final position in the CP.

MiR-22 and miR-124 Promote Radial Migration of Projection Neurons by Targeting CoREST

We further identified the miRNAs targeting CoREST in migrating projection neurons by combining two analytical approaches: (1) a transcriptional profiling of miRNAs performed on cortical extracts from WT mouse embryos at different developmental stages (Figure S4); (2) miRNA target predictions (TargetScan, MicroRNA.org, and Diana-microT V3.0 websites) to identify conserved miRNA recognition elements (MREs) in the 3′ UTR of CoREST messengers. Hence, we selected miR-22, miR-124 (Baudet et al., 2012), and miR-185 (Figures 5A and S4, see blue arrows). In situ hybridizations with locked nucleic acid (LNA)-based probes showed expression patterns compatible with CoREST modulation in distinct regions of the cortical wall of E16 embryos (Figure 5B). Indeed, miR-22 was detected at intermediate level throughout the cortical wall, whereas distributions of miR-124 and miR-185 were mostly but not only restricted to CP and VZ/SVZ, respectively (Figure 5B).

Expression levels of these miRNAs were significantly reduced in FACS-isolated Dicer$^{lox/lox}$ neurons electroporated 3 days earlier with NeuroD:Cre-GFP, as compared to controls (Figures 5C–5E). The full-length 3′ UTR of CoREST contains predicted conserved MRE sites for all selected miRNAs (Figure 5F), and we performed luciferase assays to assess the ability of these miRNAs to efficiently target CoREST. Cotransfection of a reporter plasmid expressing the *Renilla* luciferase upstream of the 3′ UTR of CoREST (3′ UTR CoREST WT) and plasmids expressing miR-22, or miR-124 specifically reduced luciferase activity in HEK293 cells (Figure 5G). Despite its bioinformatic prediction, miR-185 did not interfer with *Renilla* luciferase activity after expression of 3′ UTR CoREST WT reporter. Moreover, the 3′ UTR CoREST plasmids harboring miR-22 or miR-124 MRE point mutations (3′ UTR CoRESTmiR-22MUT and 3′ UTR CoRESTmiR-124MUT, see Figure 5G) were refractory to corresponding miRNAs in this assay, supporting the targeting specificity of the 3′ UTR of CoREST by miR-22 and miR-124 (Figure 5G). We further showed that CoREST messengers were specifically targeted in the developing cortex by endogenous miR-22 and miR-124 (Figure 5H). Altogether, these results suggest that miR-22 and miR-124 are expressed in the cortical wall where they can target the 3′ UTR of CoREST in newborn neurons.

In order to test the contribution of these miRNAs to radial migration, we performed acute electroporation of specific antagomiRs and NeuroD:GFP in the IZ of organotypic brain slices from E14 embryos to block the activity of the corresponding endogenous miRNAs (Figures 5I and S5A). The specific blockade of miR-22 or miR-124 (Figure S5A) impaired entry of electroporated neurons into the CP (Figures 5J and 5K). Coexpression of antagomiRs that neutralize both miR-22 and miR-124 did not exacerbate the migration blockade, suggesting that both miRNAs act on similar critical targets for radial migration. Electroporation of antagomiR-SCR and antagomiR-185 did not lead to migration defects and were used as controls.

We next intended to rescue the migration defect of projection neurons that lack Dicer expression, by coelectoporating mimics for miR-22 and miR-124 (alone or together; Figures 5L and 5M). Our results showed that expression of NeuroD:Cre-GFP together with either miR-22 or miR-124 mimics (or combination

Figure 3. Loss of Dicer Results in Morphological Instability during Radial Migration

Real-time imaging of NeuroD:GFP or NeuroD:Cre-GFP-expressing Dicer$^{lox/lox}$ neurons at E14 in E16 brain slices cultured for a day. Morphological changes underwent by neurons during radial migration (A). Percentage of multipolar to bipolar cell morphology conversion during 10 hr recording (B), as illustrated by a time-lapse sequence (hr) (D) or the percentage of bipolar morphology maintenance (B), as illustrated by a time-lapse sequence (hr) (E). Locomotory paths (colored dotted lines) of NeuroD:GFP or NeuroD:Cre-GFP electroporated Dicer$^{lox/lox}$ neurons recorded during time lapse imaging (F). Quantification of migration velocity (G), average pause number per 10 hr recording (H), average pause duration (I), or motility index (J) of Dicer$^{lox/lox}$ electroporated neurons at E14 with NeuroD:GFP or NeuroD:Cre-GFP vectors. Percentage of electroporated multipolar cells pausing during locomotion (L), as illustrated by a representative time-lapse sequence (hr). The red dotted line marks the position of a multipolar neuron at standstill during 3 hr, as highlighted by the thick blue line (K). CP, cortical plate; IZ, intermediate zone; VZ, ventricular zone. See also Figure S2 and Movies S1 and S2.

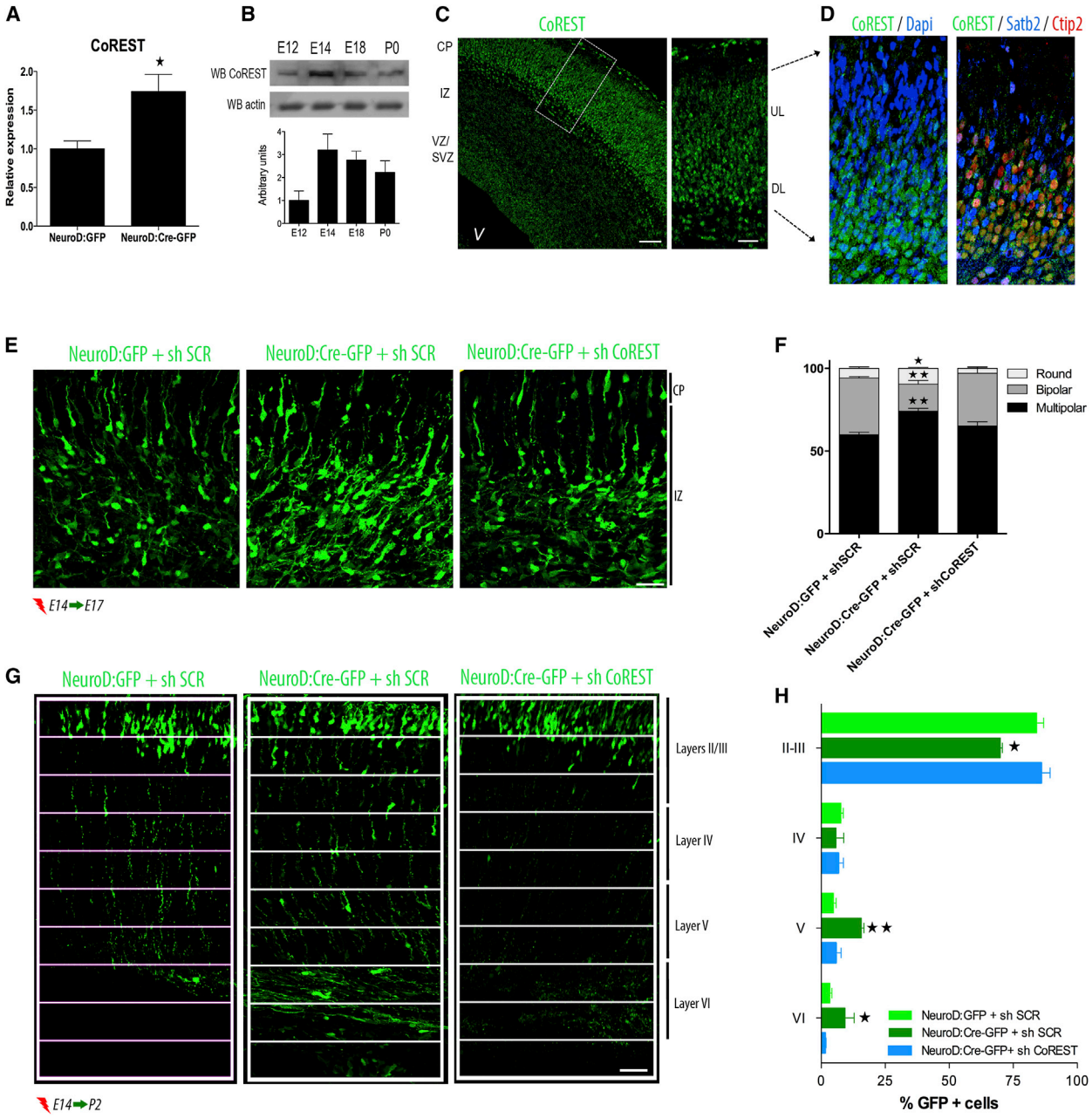

Figure 4. Deregulated Expression of CoREST Contributes to Neuronal Migration Defects in Dicer Knockout Embryos

(A and B) CoREST mRNA levels from E17 FACS-isolated NeuroD:GFP or NeuroD:Cre-GFP cortical neurons after in utero electroporation of E14 Dicer$^{lox/lox}$ embryos (A). Representative western blot of CoREST expression levels in cortical tissues from mouse embryos and pups, the quantification has been performed on three independent experiments (B).

(C and D) Immunolabelings showing the cortical distribution of CoREST (green) at E17 (C) with DAPI nuclei counterstaining (blue), Satb2 (blue), or Ctip2 (red) labelings (D). Immunolabelings in the intermediate zone showing electroporated NeuroD:GFP or NeuroD:Cre-GFP Dicer$^{lox/lox}$ neurons expressing shSCR or ShCoREST vectors at E14 and harvested at E17 (E) or P2 (G) were used for morphological analyses (F) or cortical scattering analysis (H).

CP, cortical plate; IZ, intermediate zone; VZ/SVZ, ventricular/subventricular zones; DL, deep layer; UL, upper layer. Scale bars, 100 μm (C) on the left (G) and 50 μm (C) on the right (E). See also Figure S3.

of both mimics) promoted migration in the CP to control level (NeuroD:GFP and miR-SCR-expressing neurons). Together, these results demonstrate that (1) miR-22 and miR-124 target CoREST; (2) these miRNAs are expressed in postmitotic projection neurons where they cell autonomously control radial migration.

We further performed in vivo experiments to assess the role played by the endogenous miR-22 and miR-124 during cell

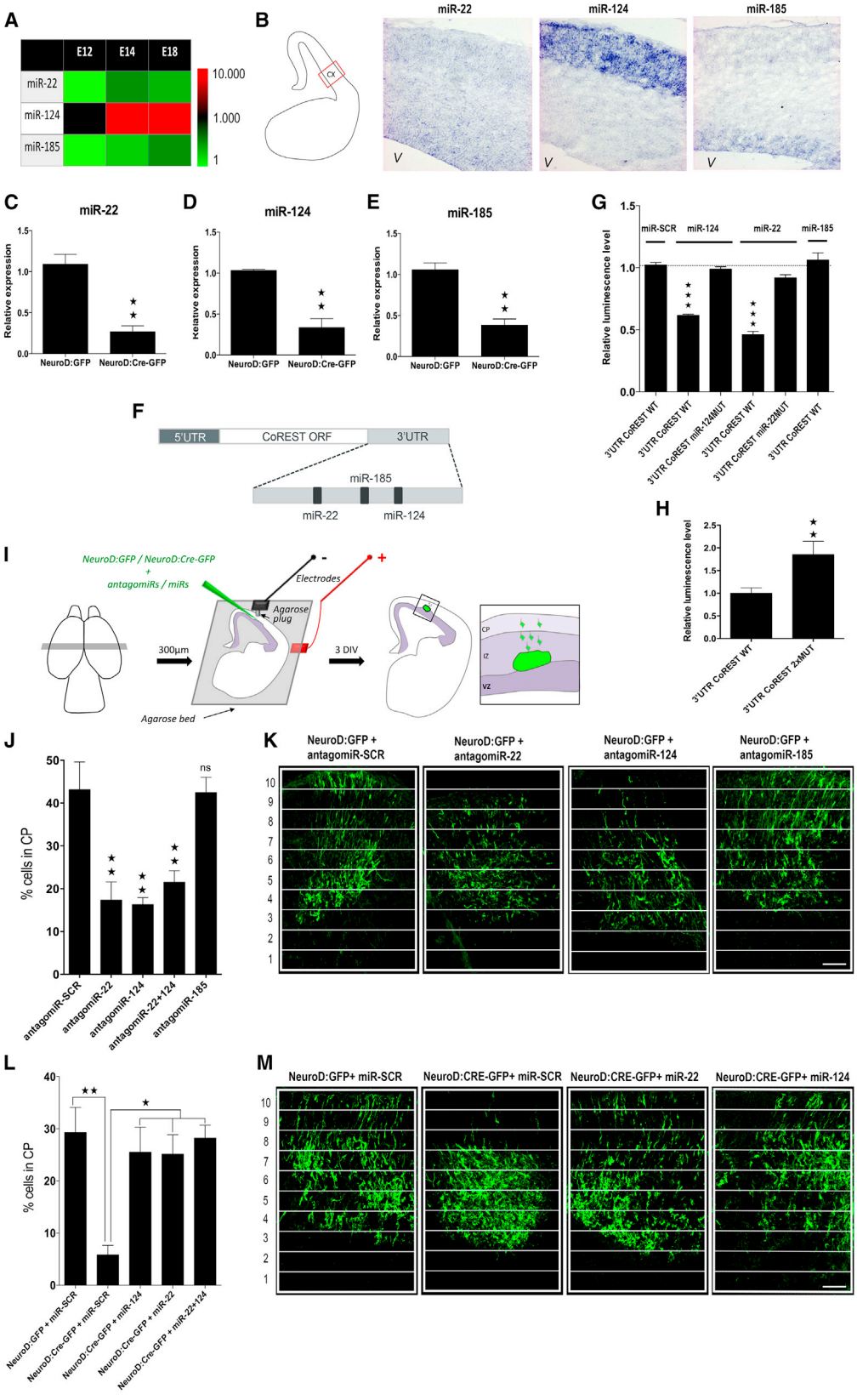

(legend on next page)

shape remodeling of migrating projection neurons. For this purpose, we electroporated E14 embryos with NeuroD-driven miRNA sponges that neutralize endogenous miR-22 or miR-124 (Figures 6A and S5C), and the analysis was conducted at E17. Electroporation of those constructs impaired radial migration (Figures 6B and 6C) and promoted accumulation of multipolar neurons at the expense of bipolar ones (Figure 6D). The effect was less pronounced with individual sponge electroporation. Live imaging was performed on cultured brain slices from E14 embryos electroporated with the sponges and further harvested at E16. Again, combining both sponge vectors impaired multipolar-bipolar neuronal conversion in the upper SVZ/lower IZ (Figure 6E) and increased the morphological instability of bipolar neurons locomoting in the upper IZ (Figure 6F). The migration defects observed after coelectroporation of both conditional sponges were comparable to those measured after genetic invalidation of Dicer in postmitotic neurons (Figures 3B and 3C). The neutralisation of endogenous miR-22 and miR-124 with the sponges resulted in accumulation of *CoREST* mRNAs, as compared to control (Figure S6B). Importantly, concurent inhibition of CoREST and expression of sponges rescued radial migration defects (Figures S6C and S6D), further supporting the critical role played by miR-22 and miR-124 to control CoREST expression during radial migration. Optochemical control of miRNA inhibition has recently been achieved in cell culture with ultraviolet (UV)-light-activated antagomiRs (Connelly et al., 2012). We further exploited optopharmacological tools to induce spatial and temporal changes of endogenous miR-22 and miR-124 activity and to further analyze the migration of projection neurons by time-lapse imaging (Figure 6G). For this purpose, cortical projection neurons from E14 embryos were coelectroporated in utero with NeuroD:GFP and caged antagomiRs that neutralize miR-22 and miR-124 after UV activation (Figure S5D). Electroporated brains were sliced 2 days later and GFP areas were subjected to UV illumination. Real-time imaging was performed 24 hr later and showed that light-activated antagomiRs reduced bipolar conversion (Figure 6I) and impaired bipolar stability (Figure 6J) of neurons navigating in the IZ, hence supporting the migration defects observed after acute slice electroporations with corresponding nonactivating antagomiRs (Figures 5J and 5K). Altogether, these results demonstrate that endogenous miR-22 and miR-124 are both required for radial migration by regulating the dynamic morphological remodeling of projection neurons. Our results also suggest that the migration phenotype resulting from the conditional removal of Dicer in postmitotic neurons mostly arise as a consequence of the lack of miR-22 and miR-124 maturation.

Accumulation of CoREST in Dicer Knockout Neurons Impedes Neuron Polarization and Migration through Transcriptional Inhibition of Doublecortin

The neuronal polarization and migration defects described above are reminiscent of those observed after acute knockdown of Dcx in cortical projection neurons (Ramos et al., 2006). Dcx is a MAP expressed by immature cortical projection neurons (Gleeson et al., 1999), which controls neuronal polarization and migration during development (Bai et al., 2003; LoTurco and Bai, 2006). Most importantly, Dcx has previously been described as a target of REST (Mandel et al., 2011). We observed a partial overlap between of Dcx and CoREST localization, but the spatial distribution of their higher expression level was inversly correlated in the cortical wall of E16 embryos (Figure 7A). A this stage, CoREST accumulated mostly in deep layers of the CP, where neurons settle into specific layers (Figures 4C and 7A). Chromatin-immunoprecipitation assays (ChIPs) performed on cortical extracts from E17 WT embryos confirmed the enrichment of REST at *Dcx* RE1 sites (Mandel et al., 2011) and demonstrated the specific recruitment of CoREST at these sites (Figure 7B). Because CoREST was detected in excess in Dicer KO projection neurons (Figure 4A), we hypothesized that its accumulation could impair *Dcx* transcription, hence leading to polarization and migration defects. To test this hypothesis, we assessed *Dcx* expression by qRT-PCR on E17 Dicer CKO postmitotic neurons (see also Figure S5B), and we detected a reduced amount of *Dcx* transcripts in Dicer CKO, as compared to the control (Figure 7C). In addition, the conditional removal of Dicer resulted in reduction of histone marks associated with active transcription (H3K9ac and H3K4m) in the *Dcx* promoter (Figures 7C and 7D). Taken together, these results suggest that the conditional loss of Dicer expression contributes to accumulation of CoREST, which further strengthens *Dcx* repression in postmitotic neurons.

The proper distribution and function of the kinesin-3 motor Kif1a requires Dcx (Liu et al., 2012). The analysis of the distribution of this Dcx downstream molecular readout in newborn projection neurons after conditional removal of Dicer or in utero expression of miR-22 and miR-124 sponge plasmids revealed an abnormal perinuclear accumulation of Kif1a at the expense of neurites (data not shown), thus further supporting a specific reduction of Dcx expression in targeted projection neurons.

Figure 5. MiR-22 and miR-124 Promote Radial Migration of Projection Neurons by Targeting CoREST

(A–H) Combination of microarray and in situ hybridization reveals miRNA candidates acting upstream CoREST. Heatmap showing the relative expression of miRNAs predicted to target CoREST in the developing cortex between E12-E18 (A). In situ hybridization performed on coronal section from wild-type E16 brains (B). Relative expression level of miR-22 (C), miR-124 (D), and miR-185 (E) in extracts from E17 FACS-isolated NeuroD:GFP or NeuroD:Cre-GFP electroporated $Dicer^{lox/lox}$ neurons at E14. Luciferase assay in HEK293 cells with vectors coding for the 3′ UTR of CoREST with or without MRE mutation (as indicated) following the luciferase gene (F) and miRNA expression vectors (as indicated) (G). Luciferase assay on E17 microdissected cortice after in utero electroporation of 3′ UTR CoREST WT or its miR-22/miR-124 targeting dead mutant (3′ UTR CoREST 2× MUT) 3 days earlier (H).

(I–M) Acute electroporation of NeuroD:GFP or NeuroDCre-GFP with antagomiR or miRNA mimics in cortical slices from E14 NMRI or $Dicer^{lox/lox}$ embryos. Technical procedure followed to express antagomiRs or miRNA mimics in $Dicer^{lox/lox}$ brain slices (I). Histograms and corresponding immunolabelings of the percentage of NMRI or $Dicer^{lox/lox}$ neurons coelectroported with NeuroD:GFP or NeuroDCre-GFP and antagomiRs (J and K) or miRNAs mimics (L and M) that reached the cortical plate (bins 9 and 10 on K and M) 3 days after electroporation in E14 brain slices. Scale bars, 100 μm in (K) and (M).

See also Figure S4.

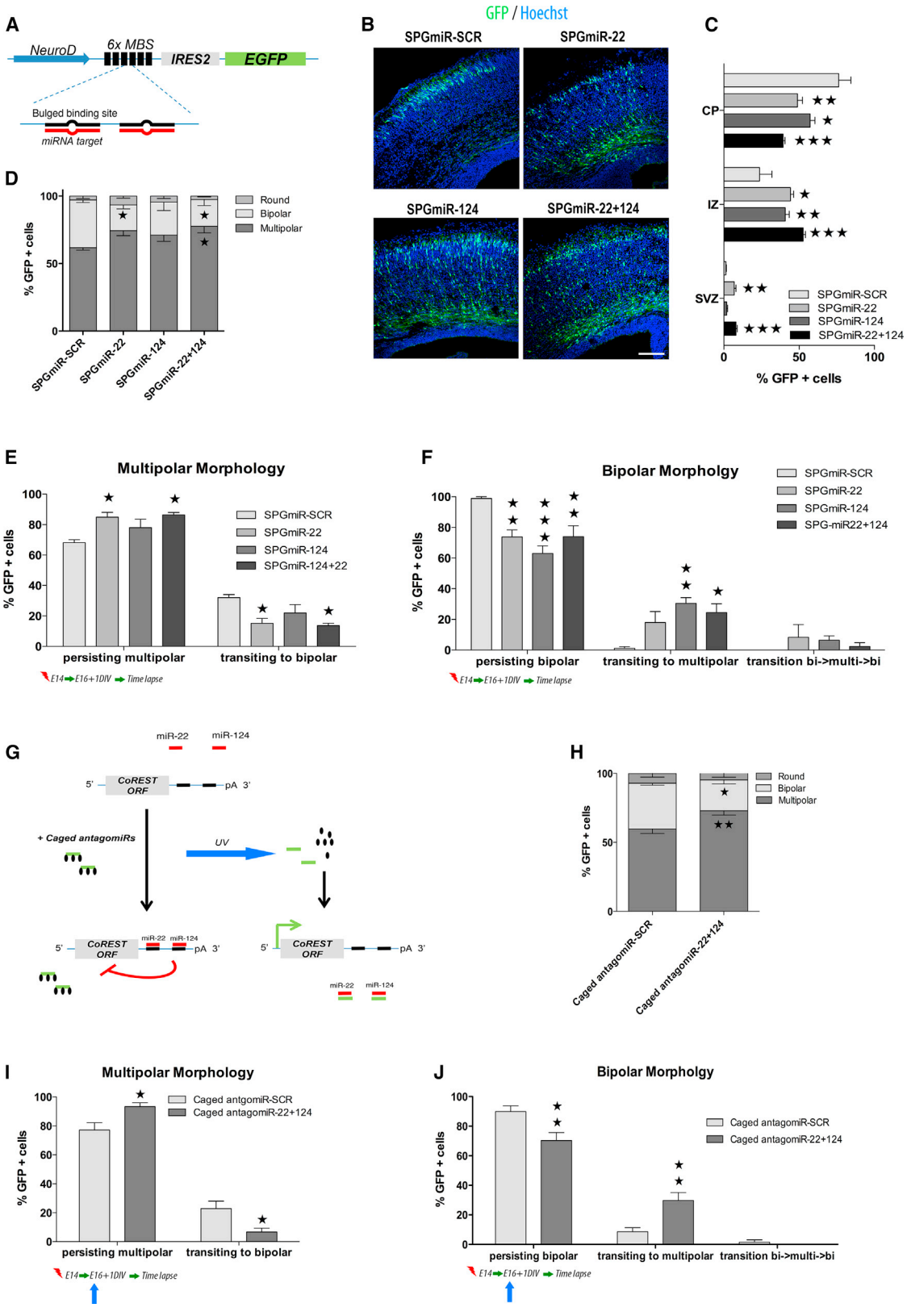

(legend on next page)

Immunolabelings performed on brain sections from E17 Dicer$^{lox/lox}$ embryos electroporated with NeuroD:Cre-GFP showed reduced Dcx staining in electroporated neurons as compared to control (NeuroD:GFP-expressing neurons; Figures 7E and 7F). Accordingly, Dcx messengers were less abundant in FACS-purified NeuroD:Cre-GFP neurons, as compared to controls (Figure 7G). Such reduction was abolished by coelectroporating NeuroD:Cre-GFP plasmids and shRNA vectors targeting CoREST (Figures 7H and S3J). We next assessed whether Dcx conditional gain of function (GOF) would rescue cell polarity and migration defects after Dicer removal. For this purpose, we performed in utero electroporation of NeuroD:GFP or NeuroD:Cre-GFP together with a vector driving Dcx expression in neurons (NeuroD:Dcx). We further performed time-lapse recordings on cultured brain slices from E16 Dicer$^{lox/lox}$ embryos that had been electroporated 2 days earlier to follow the dynamic conversion of GFP-positive neuron polarity in the IZ. Although Dcx GOF tends to increase the rate of multipolar to bipolar conversion (Figure 7I), it fully rescued the rate of bipolar persistency (Figure 7J) as well as migration velocity (Figure 7K), by preventing migration pauses in projection neurons that lack Dicer expression (Figure 7L). In addition to normalizing the dynamic polarization, Dcx rescued the final positioning of neurons in the cortex of P2 Dicer$^{lox/lox}$ animals electroporated at E14 (Figures 7M and 7N). Expression of miRNA sponge vectors that specifically target the endogenous miR-22 and miR-124 reduced expression of *Dcx* in projection neurons in vivo, as compared to control (Figure S6A). Importantly, increasing Dcx expression in postmitotic neurons thanks to electroporation of NeuroD:Dcx-GFP plasmids reverted the migration defects induced by the expression of SPGmiR-22+124 vectors in these neurons (Figures S6E and S6F). Altogether, our results highlight an epigenetic mechanism that controls the polarization and migration of postmitotic projection neurons through miR-22 and miR-124- targeting of CoREST, which fine-tunes Dcx expression, a protein that contributes to the remodeling of the MT cytoskeleton in neurons (Figure 7O).

DISCUSSION

A tight regulation of projection neuron migration is fundamental for the establishment of functional connectivity in the developing neocortex. Accumulating knowledge on the cellular and molecular regulation of cortical neuron migration has been acquired over the last decade (Heng et al., 2010). Although several genes and molecular pathways have been associated with neuronal migration in physiological or pathological conditions, the epigenetic control of this process remains poorly investigated. By combining microarrays with cell biology, we discovered that miR-22 and miR-124 are enriched in the cortical wall where they target CoREST to fine-tune expression of Dcx, thereby promoting migration to appropriate layer in the cortical plate. The present work highlights an epigenetic mechanism required during corticogenesis to dynamically regulate the polarity of migrating projection neurons.

MicroRNAs Act as Key Regulators of Radial Migration in the Developing Cortex

Accumulated work supports a critical role for miRNAs in signaling pathways that control most steps of corticogenesis (Clovis et al., 2012; Davis et al., 2008; De Pietri Tonelli et al., 2008; Gaughwin et al., 2011; Kawase-Koga et al., 2009, 2010; McLoughlin et al., 2012; Nowakowski et al., 2011; Shibata et al., 2008, 2011). However, there is currently no evidence for a direct contribution of these molecules to radial migration. Indeed, modulating miRNA expression in cortical progenitors affects survival, specification, and cell-cycle regulation that further disturbs radial migration (Volvert et al., 2012). In order to circumvent this issue, we conditionally removed Dicer in postmitotic neurons by using either NEX$^{Cre/+}$; Dicer$^{lox/lox}$ transgenic mice or in utero electroportation of Dicer$^{lox/lox}$ embryos with NeuroD:Cre-expressing vectors. Conditional removal of Dicer was combined with global gene expression profiling and miRNA expression pattern analysis, which identified miRNAs and the corresponding target gene involved in radial migration regulation. Surprisingly, we did not detect any variation of *Foxp2* expression in the cohort of electroporated projection neurons (Figure S3D) whose targeting by miRNAs has recently been associated with neuronal migration in the developing cortex (Clovis et al., 2012). This discrepancy may reflect distinct technical and conceptual approaches. Indeed, Clovis and collaborators performed in utero electroporation of *Foxp2* 3′ UTR and showed its endogenous targeting using luciferase assays. In addition, the coding sequence of *Foxp2* was expressed in cortical progenitors to mimic its lack of endogenous repression by miRNAs. Although this procedure impaired neuronal

Figure 6. Conditional Knockdown of miR-22 and miR-124 Impairs Neuronal Polarization and Migration in the Developing Cerebral Cortex

(A–F) MicroRNA sponges for miR-22 and miR-124 impair polarization and migration of projection neurons. Design of microRNA sponges driven by NeuroD promoter and containing six microRNA bulged binding sites (bulged MBS) for miR-22, miR-124, or control (SPGmiR-22, SPGmiR-124, and SPG-SCR, respectively) (A). Immunolabelings showing distributions of electroporated neurons (green) with various NeuroD-driven microRNA sponges (as illustrated) in E17 NMRI embryos electroporated at E14. Nuclei are counterstained with Hoechst 33342 (blue) (B). Corresponding neuronal scattering throughout the cortical wall of mouse embryos (C). Percentage of cortical neurons electroporated with NeuroD-driven microRNA sponges that show different morphologies in E16 NMRI mouse embryos electroporated at E14 (D). Histograms of the percentage of cortical neurons electroporated with NeuroD-driven microRNA sponges that undergo multipolar to bipolar conversion (E) or that maintained a stable bipolar morphology during migration (F) in 1 day cultured slices from corresponding brains.

(G and H) Photochemical activation of nucleobase-caged antagomiRs in postmitotic neurons migrating in cultured brain slices. UV light-activated (blue arrow) caged-antagomiRs bind to endogenous miR-22 or miR-124 and block their function in cortical neurons, leading to CoREST upregulation (G). Percentage of cortical neurons electroporated with caged antagomiRs followed by UV-light activation on brain slices that show different morphologies in E16 NMRI mouse embryos electroporated at E14 (H).

(I and J) Histogram showing the percentage of neuron with UV-light activated (blue arrow) caged-antagomiRs electroporated that undergo multipolar to bipolar conversion (I) or that maintained a stable bipolar morphology during migration (J) in 1 day cultured slices from corresponding brains.

CP, cortical plate; IZ, intermediate zone; SVZ, subventricular zone. Scale bar, 100 μm in (B). See also Figure S5.

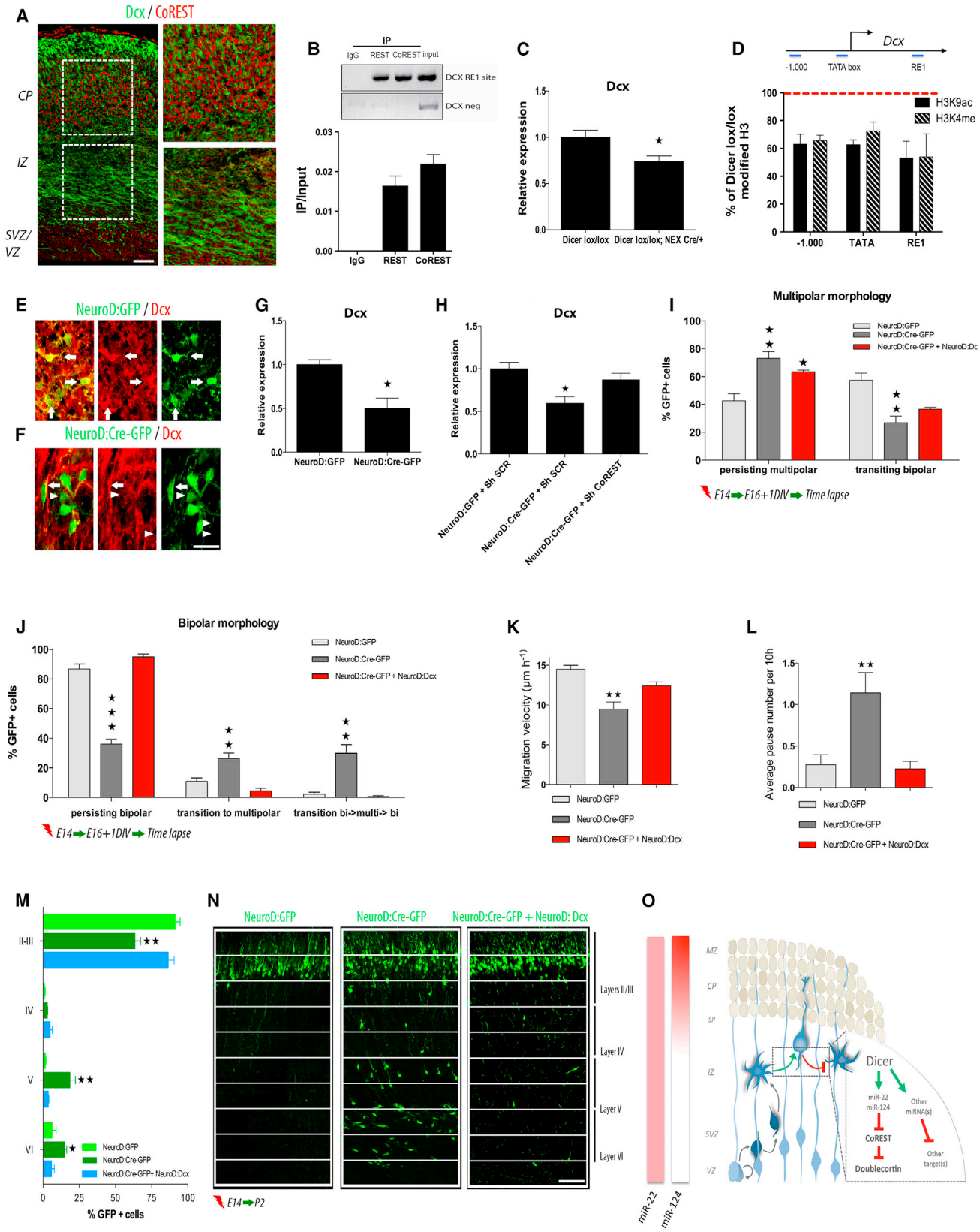

(legend on next page)

migration, it did not formaly demonstrate that repression of endogenous *Foxp2* occurs in vivo in postmitotic projection neurons to promote their migration.

MicroRNAs Fine-Tune the CoREST/Doublecortin Pathway to Control Neuronal Polarization and Radial Migration

CoREST was the only gene from our short list of regulators of neuronal polarization whose expression was upregulated in Dicer-depleted projection neurons. CoREST is a partner of the histone demethylase LSD1 in migrating projection neurons (Fuentes et al., 2012) and a component of repressor complexes that includes either REST in cortical progenitors or MeCP2 in differentiating projection neurons (Ballas et al., 2005). We showed that the conditional removal of Dicer in postmitotic projection neurons led to the upregulation of both CoREST and MeCP2, but not REST (Figures S3A and S3I). This correlates with reduction of transcriptional marks on *Dcx* as well as downregulation of its expression in cortical neurons depleted for Dicer (Figures 7C and 7D). The reduced expression of Dcx could partly account for the migration phenotype observed in Dicer-depleted neurons because this protein is a MAP that promote neuronal migration (Bai et al., 2003; Kappeler et al., 2006; Koizumi et al., 2006; Ramos et al., 2006) and whose loss of activity results in laminar heterotopia and lissencephaly in humans (des Portes et al., 1998; Gleeson et al., 1998; Sossey-Alaoui et al., 1998). Coelectroporation of NeuroD:Cre-GFP and shCoREST-encoding vectors in Dicer$^{lox/lox}$ embryos restored control levels of Dcx mRNAs (Figure 7H), supporting the existence of a direct regulation of *Dcx* by CoREST in projection neurons. Indeed, Dcx has previously been reported as a direct target of REST in cortical progenitors (Mandel et al., 2011) but not in postmitotic cortical neuron where it is released from neuronal gene chromatin (Ballas et al., 2005). This is inconsistent with our ChIP results that demonstrate a significant recruitment of both REST and CoREST to *Dcx* in postmitotic neurons (Figure 7B), suggesting that the transcriptional repressor complex composed by REST, CoREST, and likely MeCP2 (Figure S3I) targets *Dcx* in postmitotic neurons. Along this line, we demonstrated a reduction of Dcx expression after the conditional removal of Dicer in postmitotic neurons. This result contrasts with previous studies showing accumulation of Dcx in cortical neurons after genetic invalidation of Dicer in the developing cerebral cortex (Gaughwin et al., 2011; McLoughlin et al., 2012). This apparent discrepancy likely arises from the early genetic invalidation of Dicer in cortical progenitors followed by their premature differentiation into projection neurons. At the functional level, lack of Dicer disrupted radial migration at distinct steps, including multipolar-bipolar cell transition in the IZ and bipolar stability during locomotion. This phenotype was rescued after targeting CoREST or expressing Dcx in Dicer-depleted neurons. Although we cannot exclude the fine-tuning of additional targets by other miRNAs during the migration of projection neurons, the regulation of CoREST expression by miR-124 and miR-22 is a critical step for proper polarization of projection neurons during their migration in the developing cerebral cortex.

Spatial Regulation of CoREST Expression throughout the Migration Path of Projection Neurons

The expression of CoREST in the developing cortical wall results from the interplay between transcriptional and translational mechanisms, the latest including miR-22 and miR-124 (Figures 5J and 5K). Interestingly, miR-22 is expressed at intermediate levels throughout the cortical wall, whereas miR-124 accumulates mostly in the CP. These miRNAs only exhibit partial overlap in the CP where they likely cooperate to promote a tight regulation of CoREST expression and, hence, *Dcx* in order to stabilize the bipolar morphology of locomoting neurons. The molecular regulation of *Dcx* transcription also requires transcriptional activators expressed in the cortical wall (Piens et al., 2010). The dynamic expression of *Dcx* is controlled by activators and repressors, the latter including the REST/CoREST complex, which is targeted by miR-22 and miR-124. It is noteworthy that expression of CoREST is developmentaly regulated. It reaches a peak at E14 and then slowly decreases (Figure 4B) as its targeting miRNAs accumulate (Figures 5A and 4B). However, CoREST accumulates in the nucleus of Ctip2-expressing neurons (born before our electroporations) that halt migration to differentiate in deep layers of the cortex. This is surprising according to high expression of miR-124 detected in deep-layer neurons

Figure 7. Accumulation of CoREST in Dicer Knockout Neurons Impedes Neuron Polarization and Migration through Transcriptional Inhibition of Doublecortin

(A–D) CoREST controls the transcription of Dcx in migrating projection neurons. Immunolabeling of CoREST (red) and Dcx (green) on an E16 brain section. Insets are enlargement of corresponding white-boxed areas (A). Chromatin immunoprecipitation (ChIP) assay performed on cortical extracts from E17 embryos showing enrichement of REST and CoREST at Dcx RE1 sites (B). Quantification of Dcx mRNAs by qRT-PCR on E17 embryo cortical extracts, genotypes as indicated (C). ChIP showing the percentage of H3K9ac or H3K4me signal at Dcx promoter sequences (−1.000 or TATA box) or RE1 site detected on cortical extracts from E17 Dicer$^{lox/lox}$; Nex$^{Cre/+}$ as compared to Dicer $^{lox/lox}$; Nex$^{+/+}$ (control embryos). The red dotted line is the level of corresponding histone modifications detected in controls (D).

(E and F) Immunolabelings of Dcx (red) in NeuroD:GFP or NeuroD:Cre-GFP (green) electroporated Dicer$^{lox/lox}$ neurons. GFP-positive neurons harbor intense (arrow) or light (arrowhead) Dcx staining.

(G and H) Relative expression level of Dcx messengers in FACS-purified NeuroD:GFP or NeuroD:Cre-GFP from E17 Dicer$^{lox/lox}$ neurons (G) electroporated at E14 with vectors coding for shSCR or shCoREST (H).

(I–N) Percentage of cells undergoing multipolar-bipolar conversion during 10 hr recording in E16 slices cultured 1 day (I), percentage of bipolar morphology maintenance (J), migration velocity (K), average pause number (L) of neurons electroporated at E14 with combination of vectors, as indicated. Immunolabelings of sections from P2 Dicer$^{lox/lox}$ brains electroporated at E14 (GFP, green) with combination of plasmids, as indicated on the figure (N) were used for cortical scattering analysis (M).

(O) Summary scheme illustrating how Dicer and mature miRNAs control the polarization and migration of projection neurons during the establishment of the cerebral cortex.

CP, cortical plate; IZ, intermediate zone; VZ/SVZ, ventricular/subventricular zones. Scale bars, 100 μm in (A) and (N) and 5 μm in (F). See also Figure S6.

where a molecular mechanism must allow coexpression of this miRNA with CoREST. The recent discovery of endogenous miR sponges in the brain, also named RNA circles, adds a new layer of regulation that should be further investigated in this specific context (Hansen et al., 2013; Memczak et al., 2013).

EXPERIMENTAL PROCEDURES

MicroRNA Sponges

Cluster sponge elements were generated by annealing multiple oligonucleotides to obtain a sequence containing six copies of specific microRNA binding site (MBS) for miR-22, miR-124, and cel-miR-267 (control). Each sequences included mismatches at positions 10–12 to improve stability after miRNA binding: acagttcttCCGtggcagctt (for miR-22 binding site) and tggcattca GAAgtgccttaa (for miR-124 binding site), and cagtacttttGAAgagtaca (for cel-miR-267) with bulged sequence underlined (cel-miR-267). These sequences were inserted into the pCMX-Myc-IRES2EGFP (gift from X. Morin, ENS, Paris, France) digested with XhoI and SalI. These constructions allow sponge expression under pCAGGS promoter and were used to validate sponge construct by luciferase assay. Then sponges were further subcloned into pNeuroD-IRES-GFP for in vivo experiments. PITA (http://genie.weizmann.ac.il/pubs/mir07/mir07_prediction.html) and RNAHybrid (http://bibiserv.techfak.uni-bielefeld.de/rnahybrid/) were used to optimize the sequence of sponges. Algorithms predict the effectiveness of the designed binding site of the sponges by calculating free energy gained by binding to the miRNA and providing information on all other miRNAs that can potentially bind to the sponge sequence. This information was used to minimize off target miRNA binding.

Antisens Oligonucleotides, AntagomiRs

AntagomiRs (Integrated DNA technologies, Leuven, Belgium) sequences were mA*mA*mC*mA*mG*mU*mU*mC*mU*mU*mC*mA*mA*mC*mU*mG*mG*mC*mA*mG*mC*mU*mU (antagomiR-22); mA*mG*mG*mC*mA*mU*mU*mC*mA*mC*mC*mG*mC*mG*mU*mG*mC*mC*mU*mU*mA (antagomiR-124); mA*mU*mC*mA*mG*mG*mA*mA*mC*mU*mG*mC*mC*mU*mU*mU *mC*mU*mC*mU*mC*mC*mA (antagomiR-185); mA* mC*mA*mG*mU*mA*mC*mU*mU*mU*mU*mG*mU*mG*mU*mA*mG*mU*mA*mC*mA*mA (antagomiR-SCR was used as a control and targets the nonmammalian cel-miR-239). Asterisks indicate phosphorothioate bond, m indicates a 2′O-Me modified nucleotides. Light-activated 3U-caged antagomiR-22, antagomiR-124, and antagomiR-21 (for control) were synthetized by the Deiters laborator, as previously described (Connelly et al., 2012). A nucleobase-caged antagomiRs has no effect on miRNA-mediated gene silencing, until it is activated through UV-induced photochemical removal of the caging groups. Activated antagomiRs bind their corresponding endogenous miRNAs and block gene silencing function. The photocaged nucleotides 2′O-Me (6-nitropiperonyloxymethyl)-caged uridine, are underlined in antagomiR sequences (see above).

In Vivo Light Activation of AntagomiRs

pNeuroD-IRES-GFP and caged-antagomiR-22, -124, and -21 (used as a negative control) were in utero electroporated in E14 NMRI mice. Brains from E16 electroporated embryos were embedded in 3% agarose and sectioned (300 μm) with a vibratome (VT1000S, Leica). Four hours after electroporation, slices were irradiated for 1 min with a mercury lamp (Nikon C-LHGFI Intensilight) and a DAPI filter cube for excitation (Nikon A1 Eclipse Ti microscope, 40× objective, half power of the lamp). Brain slices were cultured up to 24 hr in semidry conditions (Millicell inserts, Merck Millipore), in a humidified incubator at 37°C in a 5% CO_2 atmosphere in wells containing Neurobasal medium supplemented with 1% B27, 1% N2, and 1% penicillin/streptomycin (Gibco, Life Technologies).

Cell Counting and Statistics

Cortical wall areas were identified on frozen cryostat sections according to cell density, nuclear orientation (nuclei staining with Hoescht 33342), and cell identity (immunoreactivity for ßIII-tubulin) after immunostainings, as previously described (Nguyen et al., 2006). For each sample, magnified fields (20× and 40×) were acquired on three adjacent sections with a confocal microscope to reach a cellular level of analysis. For migration experiments, 1,000–3,000 cells were counted in each brain, and three to seven brains were analyzed for each experimental condition. The cortical wall thickness was measured on Hoechst-stained sections. Statistics for dual comparisons were generated using unpaired two-tailed Student's t tests unless specified, whereas statistics for multiple comparisons were generated using one- or two-way ANOVA followed by appropriate post hoc test (GraphPad Prism software, version 5); *$p < 0.05$, **$p < 0.01$, ***$p < 0.001$ for all statistics herein (see also Table S1).

SUPPLEMENTAL INFORMATION

Supplemental Information includes Supplemental Experimental Procedures, six figures, one table, and two movies and can be found with this article online at http://dx.doi.org/10.1016/j.celrep.2014.03.075.

AUTHOR CONTRIBUTIONS

M.-L.V., P.-P.P., G.M., P.C., J.D.G., B.M., A.C., and L.N. conceived and designed the experiments. M.-L.V., P.-P.P., P.C., S.L., S.P., F.R., N.K., and J.D.G. performed the experiments. M.-L.V., P.-P.P., P.C., S.P., J.D.G., and L.N. analyzed the data. J.H., R.S., A.D., and M.M. contributed to reagents/materials. M.-L.V., J.D.G., P.-P.P., and L.N. wrote the paper.

ACKNOWLEDGMENTS

The authors thank Klaus Armin-Nave and Jean Hébert for providing cre-mouse lines and Franck Polleux, Patricio Fuentes, and Manuel Kukuljan for providing plasmids. We thank the GIGA-Imaging and Flow Cytometry platform for technical support. L.N. and P.C. are Research Associates at the Belgian National Fund for Scientific Research (F.R.S-F.N.R.S.). A.C. and B.M. are Senior Research Associate and Research Director, respectively, at the F.R.S-F.N.R.S. J.D.G. has been granted Marie Curie and EMBO long-term fellowships. L.N. is funded by grants from the F.R.S.-F.N.R.S., the Fonds Léon Fredericq, the Fondation Médicale Reine Elisabeth, and the Belgian Science Policy (IAP-VII network P7/20). L.N. and A.C. are funded by a grant from ARC (ARC11/16-01), and A.C. is funded by the Belgian Federation Against Cancer. Some scientific projects in the Nguyen and Chariot laboratories are funded by the Walloon excellence in lifesciences and biotechnology (WELBIO).

Received: December 11, 2012
Revised: October 8, 2013
Accepted: March 31, 2014
Published: May 1, 2014

REFERENCES

Abelson, J.F., Kwan, K.Y., O'Roak, B.J., Baek, D.Y., Stillman, A.A., Morgan, T.M., Mathews, C.A., Pauls, D.L., Rasin, M.R., Gunel, M., et al. (2005). Sequence variants in SLITRK1 are associated with Tourette's syndrome. Science *310*, 317–320.

Alfano, C., Viola, L., Heng, J.I., Pirozzi, M., Clarkson, M., Flore, G., De Maio, A., Schedl, A., Guillemot, F., and Studer, M. (2011). COUP-TFI promotes radial migration and proper morphology of callosal projection neurons by repressing Rnd2 expression. Development *138*, 4685–4697.

Aronica, E., Fluiter, K., Iyer, A., Zurolo, E., Vreijling, J., van Vliet, E.A., Baayen, J.C., and Gorter, J.A. (2010). Expression pattern of miR-146a, an inflammation-associated microRNA, in experimental and human temporal lobe epilepsy. Eur. J. Neurosci. *31*, 1100–1107.

Bai, J., Ramos, R.L., Ackman, J.B., Thomas, A.M., Lee, R.V., and LoTurco, J.J. (2003). RNAi reveals doublecortin is required for radial migration in rat neocortex. Nat. Neurosci. *6*, 1277–1283.

Ballas, N., Grunseich, C., Lu, D.D., Speh, J.C., and Mandel, G. (2005). REST and its corepressors mediate plasticity of neuronal gene chromatin throughout neurogenesis. Cell *121*, 645–657.

Baudet, M.L., Zivraj, K.H., Abreu-Goodger, C., Muldal, A., Armisen, J., Blenkiron, C., Goldstein, L.D., Miska, E.A., and Holt, C.E. (2012). miR-124 acts through CoREST to control onset of Sema3A sensitivity in navigating retinal growth cones. Nat. Neurosci. *15*, 29–38.

Bernstein, E., Caudy, A.A., Hammond, S.M., and Hannon, G.J. (2001). Role for a bidentate ribonuclease in the initiation step of RNA interference. Nature *409*, 363–366.

Beveridge, N.J., Gardiner, E., Carroll, A.P., Tooney, P.A., and Cairns, M.J. (2010). Schizophrenia is associated with an increase in cortical microRNA biogenesis. Mol. Psychiatry *15*, 1176–1189.

Bielas, S., Higginbotham, H., Koizumi, H., Tanaka, T., and Gleeson, J.G. (2004). Cortical neuronal migration mutants suggest separate but intersecting pathways. Annu. Rev. Cell Dev. Biol. *20*, 593–618.

Casanova, M.F., and Trippe, J., 2nd. (2006). Regulatory mechanisms of cortical laminar development. Brain Res. Brain Res. Rev. *51*, 72–84.

Chen, G., Sima, J., Jin, M., Wang, K.Y., Xue, X.J., Zheng, W., Ding, Y.Q., and Yuan, X.B. (2008). Semaphorin-3A guides radial migration of cortical neurons during development. Nat. Neurosci. *11*, 36–44.

Clovis, Y.M., Enard, W., Marinaro, F., Huttner, W.B., and De Pietri Tonelli, D. (2012). Convergent repression of Foxp2 3'UTR by miR-9 and miR-132 in embryonic mouse neocortex: implications for radial migration of neurons. Development *139*, 3332–3342.

Cobb, B.S., Nesterova, T.B., Thompson, E., Hertweck, A., O'Connor, E., Godwin, J., Wilson, C.B., Brockdorff, N., Fisher, A.G., Smale, S.T., and Merkenschlager, M. (2005). T cell lineage choice and differentiation in the absence of the RNase III enzyme Dicer. J. Exp. Med. *201*, 1367–1373.

Connelly, C.M., Uprety, R., Hemphill, J., and Deiters, A. (2012). Spatiotemporal control of microRNA function using light-activated antagomirs. Mol. Biosyst. *8*, 2987–2993.

Creppe, C., Malinouskaya, L., Volvert, M.L., Gillard, M., Close, P., Malaise, O., Laguesse, S., Cornez, I., Rahmouni, S., Ormenese, S., et al. (2009). Elongator controls the migration and differentiation of cortical neurons through acetylation of alpha-tubulin. Cell *136*, 551–564.

Davis, T.H., Cuellar, T.L., Koch, S.M., Barker, A.J., Harfe, B.D., McManus, M.T., and Ullian, E.M. (2008). Conditional loss of Dicer disrupts cellular and tissue morphogenesis in the cortex and hippocampus. J. Neurosci. *28*, 4322–4330.

De Pietri Tonelli, D., Pulvers, J.N., Haffner, C., Murchison, E.P., Hannon, G.J., and Huttner, W.B. (2008). miRNAs are essential for survival and differentiation of newborn neurons but not for expansion of neural progenitors during early neurogenesis in the mouse embryonic neocortex. Development *135*, 3911–3921.

des Portes, V., Francis, F., Pinard, J.M., Desguerre, I., Moutard, M.L., Snoeck, I., Meiners, L.C., Capron, F., Cusmai, R., Ricci, S., et al. (1998). doublecortin is the major gene causing X-linked subcortical laminar heterotopia (SCLH). Hum. Mol. Genet. *7*, 1063–1070.

Fuentes, P., Cánovas, J., Berndt, F.A., Noctor, S.C., and Kukuljan, M. (2012). CoREST/LSD1 control the development of pyramidal cortical neurons. Cereb. Cortex *22*, 1431–1441.

Gaughwin, P., Ciesla, M., Yang, H., Lim, B., and Brundin, P. (2011). Stage-specific modulation of cortical neuronal development by Mmu-miR-134. Cereb. Cortex *21*, 1857–1869.

Gleeson, J.G., Allen, K.M., Fox, J.W., Lamperti, E.D., Berkovic, S., Scheffer, I., Cooper, E.C., Dobyns, W.B., Minnerath, S.R., Ross, M.E., and Walsh, C.A. (1998). Doublecortin, a brain-specific gene mutated in human X-linked lissencephaly and double cortex syndrome, encodes a putative signaling protein. Cell *92*, 63–72.

Gleeson, J.G., Lin, P.T., Flanagan, L.A., and Walsh, C.A. (1999). Doublecortin is a microtubule-associated protein and is expressed widely by migrating neurons. Neuron *23*, 257–271.

Goebbels, S., Bormuth, I., Bode, U., Hermanson, O., Schwab, M.H., and Nave, K.A. (2006). Genetic targeting of principal neurons in neocortex and hippocampus of NEX-Cre mice. Genesis *44*, 611–621.

Gupta, A., Tsai, L.H., and Wynshaw-Boris, A. (2002). Life is a journey: a genetic look at neocortical development. Nat. Rev. Genet. *3*, 342–355.

Hansen, T.B., Jensen, T.I., Clausen, B.H., Bramsen, J.B., Finsen, B., Damgaard, C.K., and Kjems, J. (2013). Natural RNA circles function as efficient microRNA sponges. Nature *495*, 384–388.

Hattori, M., Adachi, H., Tsujimoto, M., Arai, H., and Inoue, K. (1994). Miller-Dieker lissencephaly gene encodes a subunit of brain platelet-activating factor acetylhydrolase [corrected]. Nature *370*, 216–218.

Hébert, J.M., and McConnell, S.K. (2000). Targeting of cre to the Foxg1 (BF-1) locus mediates loxP recombination in the telencephalon and other developing head structures. Dev. Biol. *222*, 296–306.

Hébert, S.S., Horré, K., Nicolaï, L., Papadopoulou, A.S., Mandemakers, W., Silahtaroglu, A.N., Kauppinen, S., Delacourte, A., and De Strooper, B. (2008). Loss of microRNA cluster miR-29a/b-1 in sporadic Alzheimer's disease correlates with increased BACE1/beta-secretase expression. Proc. Natl. Acad. Sci. USA *105*, 6415–6420.

Heng, J.I., Nguyen, L., Castro, D.S., Zimmer, C., Wildner, H., Armant, O., Skowronska-Krawczyk, D., Bedogni, F., Matter, J.M., Hevner, R., and Guillemot, F. (2008). Neurogenin 2 controls cortical neuron migration through regulation of Rnd2. Nature *455*, 114–118.

Heng, J.I., Chariot, A., and Nguyen, L. (2010). Molecular layers underlying cytoskeletal remodelling during cortical development. Trends Neurosci. *33*, 38–47.

Jimenez-Mateos, E.M., Bray, I., Sanz-Rodriguez, A., Engel, T., McKiernan, R.C., Mouri, G., Tanaka, K., Sano, T., Saugstad, J.A., Simon, R.P., et al. (2011). miRNA Expression profile after status epilepticus and hippocampal neuroprotection by targeting miR-132. Am. J. Pathol. *179*, 2519–2532.

Kappeler, C., Saillour, Y., Baudoin, J.P., Tuy, F.P., Alvarez, C., Houbron, C., Gaspar, P., Hamard, G., Chelly, J., Métin, C., and Francis, F. (2006). Branching and nucleokinesis defects in migrating interneurons derived from doublecortin knockout mice. Hum. Mol. Genet. *15*, 1387–1400.

Kawahara, H., Imai, T., and Okano, H. (2012). MicroRNAs in Neural Stem Cells and Neurogenesis. Front Neurosci. *6*, 30.

Kawase-Koga, Y., Otaegi, G., and Sun, T. (2009). Different timings of Dicer deletion affect neurogenesis and gliogenesis in the developing mouse central nervous system. Dev. Dyn. *238*, 2800–2812.

Kawase-Koga, Y., Low, R., Otaegi, G., Pollock, A., Deng, H., Eisenhaber, F., Maurer-Stroh, S., and Sun, T. (2010). RNAase-III enzyme Dicer maintains signaling pathways for differentiation and survival in mouse cortical neural stem cells. J. Cell Sci. *123*, 586–594.

Keays, D.A., Tian, G., Poirier, K., Huang, G.J., Siebold, C., Cleak, J., Oliver, P.L., Fray, M., Harvey, R.J., Molnár, Z., et al. (2007). Mutations in alpha-tubulin cause abnormal neuronal migration in mice and lissencephaly in humans. Cell *128*, 45–57.

Kim, J., Inoue, K., Ishii, J., Vanti, W.B., Voronov, S.V., Murchison, E., Hannon, G., and Abeliovich, A. (2007). A MicroRNA feedback circuit in midbrain dopamine neurons. Science *317*, 1220–1224.

Koizumi, H., Higginbotham, H., Poon, T., Tanaka, T., Brinkman, B.C., and Gleeson, J.G. (2006). Doublecortin maintains bipolar shape and nuclear translocation during migration in the adult forebrain. Nat. Neurosci. *9*, 779–786.

Lang, M.F., and Shi, Y. (2012). Dynamic Roles of microRNAs in Neurogenesis. Front Neurosci *6*, 71.

Liu, J.S., Schubert, C.R., Fu, X., Fourniol, F.J., Jaiswal, J.K., Houdusse, A., Stultz, C.M., Moores, C.A., and Walsh, C.A. (2012). Molecular basis for specific regulation of neuronal kinesin-3 motors by doublecortin family proteins. Mol. Cell *47*, 707–721.

LoTurco, J.J., and Bai, J. (2006). The multipolar stage and disruptions in neuronal migration. Trends Neurosci. *29*, 407–413.

Makeyev, E.V., Zhang, J., Carrasco, M.A., and Maniatis, T. (2007). The MicroRNA miR-124 promotes neuronal differentiation by triggering brain-specific alternative pre-mRNA splicing. Mol. Cell *27*, 435–448.

Mandel, G., Fiondella, C.G., Covey, M.V., Lu, D.D., Loturco, J.J., and Ballas, N. (2011). Repressor element 1 silencing transcription factor (REST) controls

radial migration and temporal neuronal specification during neocortical development. Proc. Natl. Acad. Sci. USA *108*, 16789–16794.

Marín, O., and Rubenstein, J.L. (2003). Cell migration in the forebrain. Annu. Rev. Neurosci. *26*, 441–483.

McKiernan, R.C., Jimenez-Mateos, E.M., Bray, I., Engel, T., Brennan, G.P., Sano, T., Michalak, Z., Moran, C., Delanty, N., Farrell, M., et al. (2012). Reduced mature microRNA levels in association with dicer loss in human temporal lobe epilepsy with hippocampal sclerosis. PLoS ONE *7*, e35921.

McLoughlin, H.S., Fineberg, S.K., Ghosh, L.L., Tecedor, L., and Davidson, B.L. (2012). Dicer is required for proliferation, viability, migration and differentiation in corticoneurogenesis. Neuroscience *223*, 285–295.

Memczak, S., Jens, M., Elefsinioti, A., Torti, F., Krueger, J., Rybak, A., Maier, L., Mackowiak, S.D., Gregersen, L.H., Munschauer, M., et al. (2013). Circular RNAs are a large class of animal RNAs with regulatory potency. Nature *495*, 333–338.

Miller, B.H., Zeier, Z., Xi, L., Lanz, T.A., Deng, S., Strathmann, J., Willoughby, D., Kenny, P.J., Elsworth, J.D., Lawrence, M.S., et al. (2012). MicroRNA-132 dysregulation in schizophrenia has implications for both neurodevelopment and adult brain function. Proc. Natl. Acad. Sci. USA *109*, 3125–3130.

Nguyen, L., Besson, A., Heng, J.I., Schuurmans, C., Teboul, L., Parras, C., Philpott, A., Roberts, J.M., and Guillemot, F. (2006). p27kip1 independently promotes neuronal differentiation and migration in the cerebral cortex. Genes Dev. *20*, 1511–1524.

Noctor, S.C., Martínez-Cerdeño, V., Ivic, L., and Kriegstein, A.R. (2004). Cortical neurons arise in symmetric and asymmetric division zones and migrate through specific phases. Nat. Neurosci. *7*, 136–144.

Nowakowski, T.J., Mysiak, K.S., Pratt, T., and Price, D.J. (2011). Functional dicer is necessary for appropriate specification of radial glia during early development of mouse telencephalon. PLoS ONE *6*, e23013.

Piens, M., Muller, M., Bodson, M., Baudouin, G., and Plumier, J.C. (2010). A short upstream promoter region mediates transcriptional regulation of the mouse doublecortin gene in differentiating neurons. BMC Neurosci. *11*, 64.

Pilz, D.T., Matsumoto, N., Minnerath, S., Mills, P., Gleeson, J.G., Allen, K.M., Walsh, C.A., Barkovich, A.J., Dobyns, W.B., Ledbetter, D.H., and Ross, M.E. (1998). LIS1 and XLIS (DCX) mutations cause most classical lissencephaly, but different patterns of malformation. Hum. Mol. Genet. *7*, 2029–2037.

Ramos, R.L., Bai, J., and LoTurco, J.J. (2006). Heterotopia formation in rat but not mouse neocortex after RNA interference knockdown of DCX. Cereb. Cortex *16*, 1323–1331.

Shi, Y., Zhao, X., Hsieh, J., Wichterle, H., Impey, S., Banerjee, S., Neveu, P., and Kosik, K.S. (2010). MicroRNA regulation of neural stem cells and neurogenesis. J. Neurosci. *30*, 14931–14936.

Shibata, M., Kurokawa, D., Nakao, H., Ohmura, T., and Aizawa, S. (2008). MicroRNA-9 modulates Cajal-Retzius cell differentiation by suppressing Foxg1 expression in mouse medial pallium. J. Neurosci. *28*, 10415–10421.

Shibata, M., Nakao, H., Kiyonari, H., Abe, T., and Aizawa, S. (2011). MicroRNA-9 regulates neurogenesis in mouse telencephalon by targeting multiple transcription factors. J. Neurosci. *31*, 3407–3422.

Sossey-Alaoui, K., Hartung, A.J., Guerrini, R., Manchester, D.K., Posar, A., Puche-Mira, A., Andermann, E., Dobyns, W.B., and Srivastava, A.K. (1998). Human doublecortin (DCX) and the homologous gene in mouse encode a putative Ca2+-dependent signaling protein which is mutated in human X-linked neuronal migration defects. Hum. Mol. Genet. *7*, 1327–1332.

Stark, K.L., Xu, B., Bagchi, A., Lai, W.S., Liu, H., Hsu, R., Wan, X., Pavlidis, P., Mills, A.A., Karayiorgou, M., and Gogos, J.A. (2008). Altered brain microRNA biogenesis contributes to phenotypic deficits in a 22q11-deletion mouse model. Nat. Genet. *40*, 751–760.

Sun, G., Ye, P., Murai, K., Lang, M.F., Li, S., Zhang, H., Li, W., Fu, C., Yin, J., Wang, A., et al. (2011). miR-137 forms a regulatory loop with nuclear receptor TLX and LSD1 in neural stem cells. Nat. Commun. *2*, 529.

Volvert, M.L., Rogister, F., Moonen, G., Malgrange, B., and Nguyen, L. (2012). MicroRNAs tune cerebral cortical neurogenesis. Cell Death Differ. *19*, 1573–1581.

Wang, X., Liu, P., Zhu, H., Xu, Y., Ma, C., Dai, X., Huang, L., Liu, Y., Zhang, L., and Qin, C. (2009). miR-34a, a microRNA up-regulated in a double transgenic mouse model of Alzheimer's disease, inhibits bcl2 translation. Brain Res. Bull. *80*, 268–273.

Westerlund, N., Zdrojewska, J., Padzik, A., Komulainen, E., Björkblom, B., Rannikko, E., Tararuk, T., Garcia-Frigola, C., Sandholm, J., Nguyen, L., et al. (2011). Phosphorylation of SCG10/stathmin-2 determines multipolar stage exit and neuronal migration rate. Nat. Neurosci. *14*, 305–313.

Willemsen, M.H., Vallès, A., Kirkels, L.A., Mastebroek, M., Olde Loohuis, N., Kos, A., Wissink-Lindhout, W.M., de Brouwer, A.P., Nillesen, W.M., Pfundt, R., et al. (2011). Chromosome 1p21.3 microdeletions comprising DPYD and MIR137 are associated with intellectual disability. J. Med. Genet. *48*, 810–818.